# Equation of State for Cold Nuclear Matter from Refractive $^{16}O + {}^{16}O$ Elastic Scattering

Dao T. Khoa,[1] W. von Oertzen,[1] H. G. Bohlen,[1] G. Bartnitzky,[2] H. Clement,[2] Y. Sugiyama,[3] B. Gebauer,[1] A. N. Ostrowski,[1] Th. Wilpert,[1] M. Wilpert,[1] and C. Langner[1]

[1]*Bereich FK, Hahn-Meitner-Institut-GmbH, Glienicker Strasse 100, D-14109 Berlin, Germany*
[2]*Physikalisches Institut, Universität Tübingen, Auf der Morgenstelle 14, D-72076 Tübingen, Germany*
[3]*Advanced Science Research Center, JAERI, Tokai-mura, Ibaraki-ken 319-11, Japan*
(Received 19 August 1994)

The nuclear density overlap, which occurs during refractive heavy-ion scattering, opens an alternative approach to study the equation of state (EOS) for cold nuclear matter. For this purpose elastic $^{16}O + {}^{16}O$ scattering at incident enegies of 145, 250, 350, and 480 MeV has been measured very accurately, up to large angles. A systematic folding analysis of these data has been performed using an effective density dependent interaction based on the $G$-matrix elements of the Paris nucleon-nucleon potential. We find, with the observed refractive scattering patterns, that a soft EOS (with the nuclear incompressibility $K$ around 200 MeV) is the most realistic one.

PACS numbers: 25.70.Bc, 21.65.+f, 24.10.Ht

One of the main goals of the study of heavy-ion (HI) reactions remains the determination of the nuclear equation of state (EOS), which is important in both nuclear physics and astrophysics. Different types of the EOS are usually distinguished by different values of the nuclear incompressibility $K$. Many attempts in this direction have been made in the study of high-energy central HI collisions, where one hopes to deduce from the measured transverse flows or various particle (and nuclear fragment) spectra some information on the EOS. Various transport models [1] are successfully used in reproducing such data, but the results obtained so far remain inconclusive [2] concerning the EOS. Another method is the determination of the incompressibility $K$ from the observed nuclear monopole resonances [3–5]. However, a recent study [5] still shows rather large uncertainties in the $K$ values.

In general, we need a well-defined (and sensitive to $K$) quantity which can be measured with high precision. We need further an effective nucleon-nucleon (*NN*) interaction which reproduces, on the one hand, the basic nuclear matter properties (like the saturation energy and density), and, on the other hand, can be used as a basic input in the description of the considered experimental quantity. With this interaction one should be able to generate different $K$ values by varying parameters of the (density dependent) interaction [6,7], so that one can directly test the sensitivity of the considered quantity to the EOS.

In this Letter we show that a high-precision study of refractive HI scattering can be an alternative method to determine the nuclear incompressibility $K$. For this purpose, a consistent set of elastic $^{16}O + {}^{16}O$ scattering data at $E_{\rm lab} = 145$ MeV (by Sugiyama *et al.* [8]) and at 250, 350, and 480 MeV (by using the Q3D magnetic spectrometer at the cyclotron at Hahn-Meitner-Institut Berlin [9–11]) has been measured. These data cover a wide angular range, down to very small cross sections where the ratio $d\sigma/d\sigma_{\rm Mott}$ reaches $10^{-5}$. Details about the measurements can be found in Refs. [8–11], the data at 145 and 350 MeV (reported first in Refs. [8] and [9]) have been remeasured at certain angular ranges. The optical model (OM) analysis has been made using the $^{16}O + {}^{16}O$ potentials calculated within a generalized double-folding model [7].

For use in the folding model, a realistic density dependence is introduced into the effective interaction [12] derived from the $G$-matrix elements of the Paris *NN* potential (denoted hereafter as the M3Y-Paris interaction). The parameters of the density dependence are chosen [6] so that in a simple Hartree-Fock calculation one obtains a good description of the normal nuclear matter. With the direct ($v_D$) and exchange ($v_{EX}$) parts determined from the singlet and triplet even ($v_{SE}, v_{TE}$) and odd ($v_{SO}, v_{TO}$) components of the M3Y-Paris forces

$$v_D(r) = 11\,061.625\frac{\exp(-4r)}{4r} - 2537.5\frac{\exp(-2.5r)}{2.5r}, \tag{1a}$$

$$v_{EX}(r) = -\,1524.25\frac{\exp(-4r)}{4r} - 518.75\frac{\exp(-2.5r)}{2.5r} - 7.8474\frac{\exp(-0.7072r)}{0.7072r}, \tag{1b}$$

the density- (and energy-) dependent interaction is

$$v_{D(EX)}(\rho, E, r) = F(\rho)g(E)v_{D(EX)}(r). \tag{2}$$

Here $g(E) = 1 - 0.003E$, where $E$ is the incident energy per nucleon. The explicit form of the density-dependent factor $F(\rho)$ is given by Eq. (3) in Ref. [7]. The linear energy dependent factor $g(E)$ in Eq. (2) is introduced, as in Ref. [6], for a full agreement with the empirical energy dependence of the nucleon optical potential. The nuclear incompressibility $K$ can be determined [6] as the curvature of the binding energy of cold nuclear matter at the saturation density $\rho_0$. While giving the same description of cold nuclear matter at $\rho_0$, different

 0031-9007/95/74(1)/34(4)$06.00 

TABLE I. Parameters [see Eq. (3) in Ref. [7]] of different density-dependences [$F(\rho)$] of the M3Y-Paris interaction. The nuclear incompressibilities $K$ were obtained from a Hartree-Fock calculation [6].

| Interaction | $C$ | $\alpha$ | $\beta$ | $K$ (MeV) |
|---|---|---|---|---|
| DDM3Y1 | 0.2963 | 3.7231 | 3.7384 fm$^3$ | 176 |
| BDM3Y1 | 1.2521 | 1.7452 fm$^3$ | 1.0 | 270 |
| BDM3Y2 | 1.0664 | 6.0296 fm$^6$ | 2.0 | 418 |
| BDM3Y3 | 1.0045 | 25.115 fm$^9$ | 3.0 | 566 |

density-dependent parameters generate different $K$ values, i.e., different nuclear EOS (see Table I).

We note that in the new version [7] of the folding model the exchange potential is evaluated within a local density formalism, using the *finite-range* exchange interaction (1b). This is a much better approximation as compared to the *zero-range* pseudopotential adopted in earlier folding calculations [13,14]. Since the original M3Y-Paris interaction [Eqs. (1)] is real, the folded potential is used further as the real part of the HI optical potential. The imaginary part is assumed to have Woods-Saxon (WS) form supplemented with a surface (WSD) term [see Eq. (16) in Ref. [7]]. The renormalization factor $N_R$ of the folded potential and the parameters of the imaginary potential are adjusted to a best fit of the data. The $^{16}$O density is taken as a Fermi distribution with parameters chosen [15] to reproduce the shell-model density. The Coulomb potential is generated by folding two uniform charge distributions for $^{16}$O with a radius of 3.54 fm. All OM calculations were made using the code PTOLEMY [16].

A renormalization of the folded potential is necessary to account roughly for high-order effects [13]. These effects are not strong for the $^{16}$O + $^{16}$O system, and we expect the best-fit values of $N_R$ obtained with the M3Y-Paris interaction to be slightly smaller than unity, like those obtained earlier [7] with the M3Y interaction based on the Reid *NN* potential (M3Y Reid). Note that in our folding analysis the shape of the real potential over a large range of internuclear distances is fixed by the choice of the density-dependent interaction. We find that all the calculated potentials are close in strength at the surface region which corresponds to the small overlap density (Fig. 1). The main difference between different types of the folded potential is showing up at smaller distances which correspond to larger ($\rho > \rho_0$) overlap densities (see the direct and exchange parts of different folded potentials for the $^{16}$O + $^{16}$O system at 250 MeV plotted in the upper and middle panels of Fig. 1, respectively). Because of the different radial shapes of the M3Y-Paris and M3Y-Reid interactions, one has a very different behavior of the direct and exchange potentials in two cases (see also Figs. 2 and 5 from Ref. [7]). However, the total potentials are quite close in both cases, a fact showing the reliability of the new folding approach [7].

Results of our folding analyses are presented in Fig. 2 and Table II. These elastic $^{16}$O + $^{16}$O data, with a clear refractive pattern at large angles, allow the observation of the contributions from small partial waves, which in turn are determined by the scattering potential at small distances [9,10]. A rather weak absorption has been found for this system [7,9,10,17], which is clearly due to the double closed-shell structure of the $^{16}$O nucleus. As can be seen, the DDM3Y1 and BDM3Y1 potentials turn out to be the most appropriate ones which give the best description to the data in the whole angular and energy range. Note that the $\chi^2$ values obtained for the data at 250, 350, and 480 MeV (Table II) are determined mainly by the fit to the data points in the diffraction region. The difference

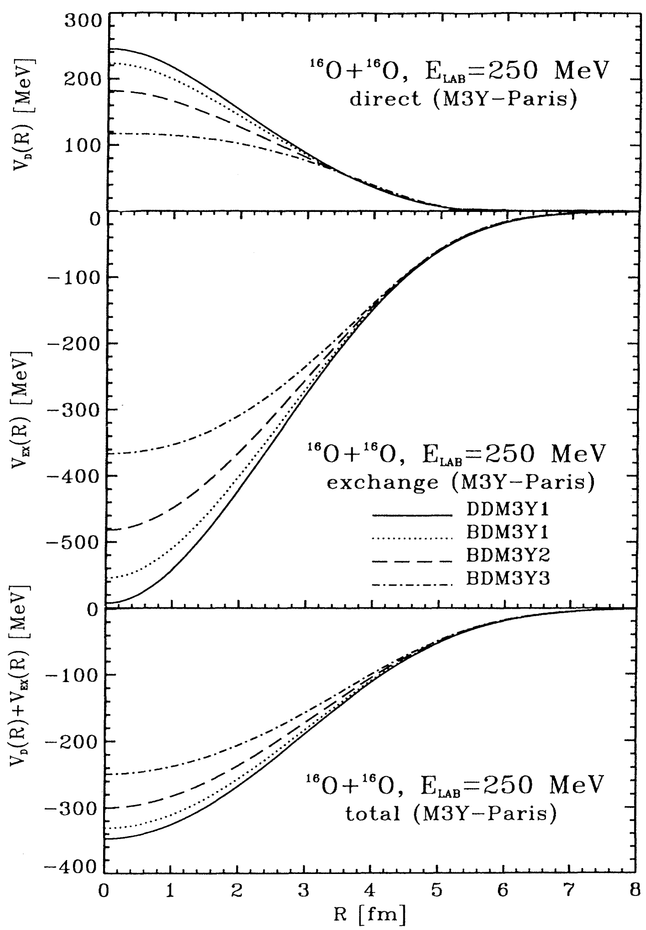


FIG. 1. Direct (upper panel) and exchange (middle panel) parts of the total $^{16}$O + $^{16}$O folded potentials (lower panel) at 250 MeV, calculated using different density-dependent interactions (Table I).

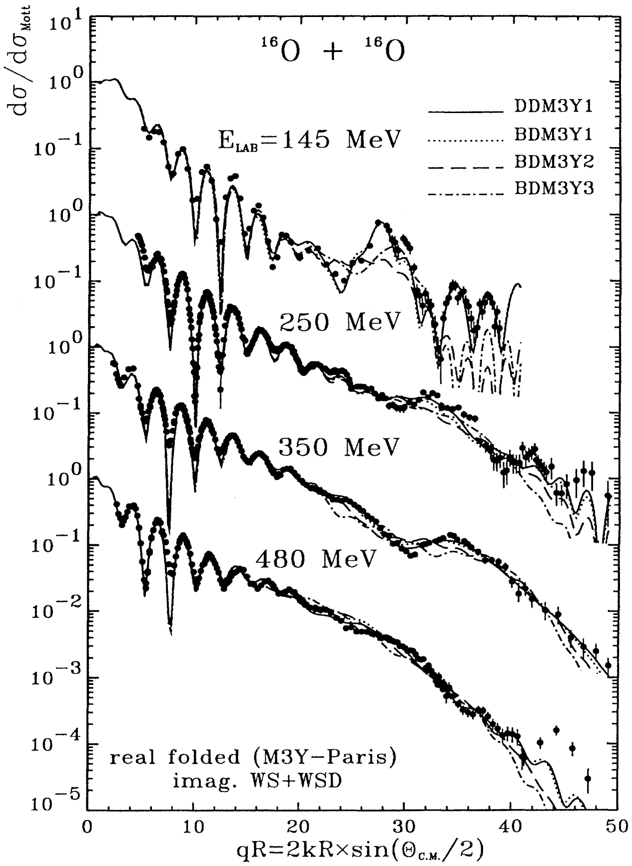


FIG. 2. Fits to the elastic $^{16}$O + $^{16}$O scattering data at $E_{\mathrm{lab}} =$ 145, 250, 350, and 480 MeV given by different types of the optical potential. The real folded potentials were calculated using different density-dependent interactions (Table I) and the imaginary potentials were fitted in the WS+WSD shape (Table II). $q$ is the linear momentum transfer and $R = 2 \times 16^{1/3}$ fm.

in the $\chi^2$ value for different potentials would have been more drastic in favor of the DDM3Y1 and BDM3Y1 potentials (like that found for the 145 MeV data), if there had been more data points at large angles (which are extremely difficult to measure). In Fig. 2 the calculated cross sections and the data are plotted vs $qR$, where $q$ is the linear momentum transfer and $R = 2 \times 16^{1/3}$ fm. From this plot we observe two remarkable facts.

(a) The diffractive part of the scattering cross section, which is produced by an interference between the near and far side components of the scattering amplitude, changes very little in the energy range up to 30 MeV/nucleon. This applies to the *position of the diffraction structure* as well as to its *absolute magnitude*. This part mainly reflects the *radius* of the semitransparent nucleus and the *width* of the surface region. If one uses the famous Blair's formula for the "black disk" scattering, the diffractive pattern (plotted vs $qR$) would be the same at all energies.

(b) The refractive part (at large $\Theta$ or $qR$ values) can be clearly distinguished from the diffractive structure, it is shifting substantially towards small angles with increasing incident energy. The first Airy (or rainbow) minimum is observed in the data at 350 MeV [7,9,10] at $qR \simeq 30$ ($\Theta_{\mathrm{c.m.}} \simeq 44°$). At 250 MeV it is located at $qR \simeq 40$ ($\Theta_{\mathrm{c.m.}} \simeq 70°$), and at 480 MeV it is shifted to $qR \simeq 24$ ($\Theta_{\mathrm{c.m.}} \simeq 30°$). While the rainbow maximum preceding this Airy minimum is destroyed by the Mott interference at 250 MeV, it moves rather close to the diffraction region at 480 MeV. The data at 145 MeV [8], remeasured recently to angles beyond 90°, have a clear maximum centered around $qR \simeq 37.5$ ($\Theta_{\mathrm{c.m.}} \simeq 90°$), which can be shown to be a remnant of the second Airy maximum (see Fig. 13 from Ref. [7]). It is remarkable that the two subsequent maxima at $\Theta_{\mathrm{c.m.}} \simeq 82°$ and 90° with $d\sigma/d\sigma_{\mathrm{Mott}}$ of about $10^{-3}$, predicted by the best-fit DDM3Y1 and BDM3Y1 potentials obtained with the M3Y-Reid interaction [7], have been observed later in the experiment. We recall that the refractive part, dominated by the far side component of the scattering amplitude, can be shown [18] to be sensitive to the real HI potential at small radii. Thus the shape of the measured $^{16}$O + $^{16}$O elastic cross sections at large angles is essential to test different real folded potentials.

Even though some difference in the real potentials can be compensated by a more flexible form of the imaginary potential, the inclusion of the surface (WSD) term, which has been proven necessary [7,10] in reproducing the data at 350 MeV with a folding-type real potential, does not improve much the fits given by the BDM3Y2 and BDM3Y3 potentials. The renormalization of about 10% of the real folded potential, mainly fixed by the data points in the diffraction region, leads to about the same values of different folded potentials at $R \simeq 5-6$ fm, and the relative difference in the shape caused by different $F(\rho)$ (lower panel of Fig. 1) remains practically the same.

With the density-dependent and exchange effects taken into account accurately, the energy dependence of the $^{16}$O + $^{16}$O potential is rather well predicted. For a consistent description of the elastic $^{16}$O + $^{16}$O data at incident energies from about 10 to 30 MeV/nucleon, one obtains the best fit $N_R = 0.86 \pm 0.04$ (for the DDM3Y1 potential), which gives volume integrals per interacting nucleon pair ($-J_R$) decreasing from 340 to 260 MeV fm$^3$ (see Table II). We find that within the considered energy range, the $N_R$ values slightly decrease with the increasing energy, an effect which could be due to the opening of more inelastic channels as the incident energy increases. We note that the DDM3Y1 and BDM3Y1 density dependences are quite close to the realistic density dependence [19] obtained from an earlier analysis of proton and light-ion ($d$, $^3$He, and $^4$He) scattering at 20–30 MeV/nucleon. Thus, both heavy- and light-ion data consistently demand a rather weak density dependence of the effective $NN$ interaction, which in turn favors a soft EOS.

In conclusion, the elastic $^{16}$O + $^{16}$O scattering data at $E_{\mathrm{lab}} = 145$, 250, 350, and 480 MeV have been measured and analyzed within the OM using the density-dependent folding potential. For this purpose, a realistic density dependence was introduced into the M3Y-Paris interaction.

TABLE II. OM parameters used in the folding analysis of the elastic $^{16}$O + $^{16}$O data at $E_{\rm lab}$ = 145, 250, 350, and 480 MeV [see Eq. (16) in Ref. [7], with $R_{V(D)} = 2r_{V(D)}16^{1/3}$]. $\chi^2$ values were obtained with uniform 10% errors.

| Potential | $N_R$ | $-J_R$ (MeV fm$^3$) | $\langle r_R^2\rangle^{1/2}$ (fm) | $W_V$ (MeV) | $r_V$ (fm) | $a_V$ (fm) | $W_D$ (MeV) | $r_D$ (fm) | $a_D$ (fm) | $\sigma_R$ (mb) | $\chi^2$ |
|---|---|---|---|---|---|---|---|---|---|---|---|
| $^{16}$O + $^{16}$O, $E_{\rm lab}$ = 145 MeV | | | | | | | | | | | |
| DDM3Y1 | 0.906 | 338 | 4.170 | 10.62 | 1.13 | 0.768 | 12.58 | 1.04 | 0.515 | 1650 | 9.8 |
| BDM3Y1 | 0.932 | 337 | 4.175 | 11.36 | 1.13 | 0.830 | 11.42 | 1.03 | 0.513 | 1708 | 11.3 |
| BDM3Y2 | 0.947 | 326 | 4.192 | 24.30 | 1.13 | 0.633 | 10.68 | 1.03 | 0.353 | 1598 | 35.0 |
| BDM3Y3 | 0.972 | 313 | 4.245 | 13.04 | 1.13 | 0.778 | 16.19 | 1.03 | 0.427 | 1655 | 29.6 |
| $^{16}$O + $^{16}$O, $E_{\rm lab}$ = 250 MeV | | | | | | | | | | | |
| DDM3Y1 | 0.860 | 305 | 4.176 | 31.30 | 1.00 | 0.675 | 4.251 | 1.17 | 0.578 | 1664 | 7.0 |
| BDM3Y1 | 0.875 | 302 | 4.180 | 31.87 | 1.00 | 0.711 | 3.919 | 1.16 | 0.565 | 1673 | 7.6 |
| BDM3Y2 | 0.899 | 295 | 4.198 | 34.26 | 1.00 | 0.751 | 3.076 | 1.17 | 0.522 | 1692 | 9.4 |
| BDM3Y3 | 0.923 | 283 | 4.252 | 36.00 | 1.00 | 0.736 | 2.802 | 1.17 | 0.548 | 1689 | 10.2 |
| $^{16}$O + $^{16}$O, $E_{\rm lab}$ = 350 MeV | | | | | | | | | | | |
| DDM3Y1 | 0.878 | 298 | 4.181 | 26.44 | 1.13 | 0.661 | 6.245 | 0.94 | 0.366 | 1639 | 4.8 |
| BDM3Y1 | 0.894 | 294 | 4.186 | 27.58 | 1.13 | 0.649 | 3.805 | 0.97 | 0.341 | 1633 | 5.4 |
| BDM3Y2 | 0.918 | 288 | 4.204 | 28.72 | 1.13 | 0.638 | 1.372 | 1.08 | 0.280 | 1628 | 7.1 |
| BDM3Y3 | 0.943 | 276 | 4.258 | 26.21 | 1.13 | 0.641 | 3.580 | 1.11 | 0.360 | 1621 | 8.6 |
| $^{16}$O + $^{16}$O, $E_{\rm lab}$ = 480 MeV | | | | | | | | | | | |
| DDM3Y1 | 0.818 | 261 | 4.188 | 32.13 | 1.06 | 0.762 | 1.743 | 0.97 | 0.216 | 1655 | 5.2 |
| BDM3Y1 | 0.833 | 258 | 4.193 | 31.52 | 1.06 | 0.779 | 1.843 | 0.98 | 0.225 | 1674 | 5.6 |
| BDM3Y2 | 0.856 | 252 | 4.212 | 30.23 | 1.06 | 0.793 | 1.940 | 1.03 | 0.339 | 1683 | 7.0 |
| BDM3Y3 | 0.879 | 242 | 4.266 | 28.87 | 1.06 | 0.818 | 2.125 | 1.09 | 0.334 | 1707 | 8.6 |

The results show that both the diffractive and refractive parts of the angular distribution can be consistently described only by a folding potential built upon an effective *NN* interaction which gives a rather *soft* EOS for the cold nuclear matter, with $K \simeq 170-270$ MeV. This result does not depend on the specific form of the chosen *NN* forces, because the same results were obtained [7] with the density-dependent M3Y-Reid interaction. Our conclusion is in agreement with some models of supernova explosions [20] where $K$ values around 200 MeV are suggested.

We thank Ray Satchler for helpful comments and interest in the present study.

[1] G.F. Bertsch and S. Das Gupta, Phys. Rep. **160**, 198 (1988); W. Cassing, V. Metag, U. Mosel, and N. Nitta, *ibid.* **188**, 363 (1990); J. Aichelin, *ibid.* **202**, 233 (1991).
[2] G.D. Westfall *et al.,* Phys. Rev. Lett. **71**, 1986 (1993).
[3] J.P. Blaizot, Phys. Rep. **64**, 171 (1980).
[4] A. van der Woude, Prog. Part. Nucl. Phys. **18**, 217 (1987).
[5] S. Shlomo and D.H. Youngblood, Phys. Rev. C **47**, 529 (1993).
[6] Dao T. Khoa and W. von Oertzen, Phys. Lett. B **304**, 8 (1993).
[7] Dao T. Khoa, W. von Oertzen, and H.G. Bohlen, Phys. Rev. C **49**, 1652 (1994).
[8] Y. Sugiyama, Y. Tomita, H. Ikezoe, Y. Yamanouchi, K. Ideno, S. Hamada, T. Sugimitsu, M. Hijiya, and Y. Kondo, Phys. Lett. B **312**, 35 (1993).
[9] E. Stiliaris, H.G. Bohlen, P. Fröbrich, B. Gebauer, D. Kolbert, W. von Oertzen, M. Wilpert, and Th. Wilpert, Phys. Lett. B **223**, 291 (1989).
[10] H.G. Bohlen, E. Stiliaris, B. Gebauer, W. von Oertzen, M. Wilpert, Th. Wilpert, A. Ostrowski, Dao T. Khoa, A.S. Demyanova, and A.A. Ogloblin, Z. Phys. A **346**, 189 (1993).
[11] G. Bartnitzky, Ph.D. thesis, University of Tübingen, 1994.
[12] N. Anantaraman, H. Toki, and G.F. Bertsch, Nucl. Phys. **A398**, 269 (1983).
[13] G.R. Satchler and W.G. Love, Phys. Rep. **55**, 183 (1979).
[14] A.M. Kobos, B.A. Brown, P.E. Hodgson, G.R. Satchler, and A. Budzanowski, Nucl. Phys. **A384**, 65 (1982); M.E. Brandan and G.R. Satchler, *ibid.* **A487**, 477 (1988).
[15] M. El-Azab Farid and G.R. Satchler, Nucl. Phys. **A438**, 525 (1985).
[16] M.H. Macfarlane and S.C. Pieper, Argonne National Laboratory Report No. ANL-76-11 (1978).
[17] M.E. Brandan and G.R. Satchler, Phys. Lett. B **256**, 311 (1991); Y. Kondo, F. Michel, and G. Reidemeister, *ibid.* **242**, 340 (1990).
[18] G.R. Satchler, Nucl. Phys. **A409**, 3c (1983).
[19] M. Ermer, H. Clement, G. Frank, P. Grabmayr, and G.J. Wagner, Phys. Lett. B **224**, 40 (1989); N. Heberle, H. Clement, M. Ermer, P. Grabmayr, M. Hammens, R. Henneck, and I. Sick, *ibid.* **250**, 15 (1990).
[20] E.D. Baron, J. Cooperstein, and S. Kahana, Nucl. Phys. **A440**, 744 (1985).